X-652-72-312
PREPRINT

NASA TM X-66006

MICROWAVE SIGNATURES OF FIRST-YEAR AND MULTIYEAR SEA ICE

P. GLOERSEN
W. NORDBERG
T. J. SCHMUGGE
T. T. WILHEIT
W. J. CAMPBELL

AUGUST 1972

GSFC
GODDARD SPACE FLIGHT CENTER
GREENBELT, MARYLAND

ORIGINAL CONTAINS
COLOR ILLUSTRATIONS

22p

X-652-72-312

MICROWAVE SIGNATURES OF FIRST-YEAR AND MULTIYEAR SEA ICE

P. Gloersen
W. Nordberg
T. J. Schmugge
T. T. Wilheit
Goddard Space Flight Center

W. J. Campbell
Ice Dynamics Project
U. S. Geological Survey

August 1972

GODDARD SPACE FLIGHT CENTER
Greenbelt, Maryland

MICROWAVE SIGNATURES OF FIRST-YEAR AND MULTIYEAR SEA ICE

P. Gloersen, W. Nordberg, T. J. Schmugge, and T. T. Wilheit

NASA Goddard Space Flight Center

and

W. J. Campbell

Ice Dynamics Project, U.S. Geological Survey

ABSTRACT

A combination of remote sensing from an aircraft and simultaneous surface measurements have confirmed the feasibility of identifying old and new sea ice according to its emission of thermal radiation at wavelengths between 0.3 and 3 cm. Emissivity of first-year thick ice with a surface temperature of about 260 K is 0.95 or greater for wavelengths between 0.81 and 11 cm; the emissivity of multiyear ice is 0.8 at 0.81 cm and 0.95 at 11 cm, increasing monotonically in this wave length interval. The ease with which multiyear ice can be distinguished from first-year ice using a passive microwave radiometer is demonstrated by comparing mosaics prepared both from photographs and images of 1.55 cm radiation.

MICROWAVE SIGNATURES OF FIRST-YEAR AND MULTIYEAR SEA ICE

INTRODUCTION

A recent study (Wilheit, et al. 1971) of the microwave radiation from sea ice north of Pt. Barrow, Alaska, has indicated that the emissivity can vary significantly according to ice types. Microwave emissivities, photographs, and laser profilometer data were related to two classifications of large ice areas: one year or younger and multiyear ice floes. These classifications were consistent with simultaneous visual observations also made from the aircraft. In terms of microwave signatures, two distinct ice types existed in that region during the late Spring, when the average ice temperature integrated vertically is at its annual coldest, low emissivity ice which was visually identified as multiyear ice, and high emissivity ice which corresponded to first-year or younger ice.

These correlations established in that study, however, were tentative, both because of the absence of surface-based observations and because the observations appeared to be in conflict with theoretical predictions of ice emissivity as a function of age (Hoekstra and Cappillino 1971, Stogryn 1971). According to that theory, the microwave emissivity of first-year ice should decrease rapidly as temperature increases to the melt point. Yet, the ice surface temperatures measured with an infrared radiometer on board the aircraft during that study was uniformly 274 ±2 K. Also, the incipient water ponds, the wet ice, and the

general melting which were encountered during the Wilheit et al. (1971) study raised questions regarding the validity of the reported correlations of microwave brightness temperatures with the age of the ice.

Basharinov, et al. (1971) reported observations from the Cosmos 243 satellite and indicated that the microwave brightness temperature of sea ice depends on its thermometric temperature, compaction, thickness, skin depth, and temperature profile. They distinguish between the brightness temperatures at various wavelengths of continental glaciers, ice shelves, and sea ice. Although they discuss radiometric data acquired over both polar regions, they did not report any contrasts between the microwave signatures of first-year and multiyear sea ice present in the Arctic region. For these reasons, we conducted airborne measurements of the microwave emission from Arctic sea ice combined with extensive surface based measurements obtained partly by one of us (Campbell) and partly by others with the Arctic Ice Dynamics Joint Experiment (AIDJEX). Also, these measurements were made under conditions of much lower surface temperatures. The results from these measurements and their interpretations are reported here.

DESCRIPTION OF EXPERIMENT

The instruments used for these measurements are listed in Table I. For the most part, they have been described elsewhere, as indicated in Table I. These instruments were flown on the NASA Convair 990 aircraft laboratory. Measurements were made at several different altitudes. At the high altitude,

10 km, a five-track grid pattern was flown so as to obtain a synoptic view of a macroscale area of sea ice. Measurements at 1.55 cm wavelength obtained during these runs were used to prepare a mosaic of radiometric images in false-color format to present a pictorial view of the area surrounding the AIDJEX site, where surface data were acquired. Infrared Ektachrome photographs were also taken during these runs from which a photomosaic of the area was obtained. Essential for this portion of the experimentation was the inertial navigation system on board the aircraft which permitted absolute positioning of the grid lines to within about 1.6 km.

The lower altitude runs, at about 0.8 km, were used to correlate the high precision multispectral radiometric measurements with ice characteristics observed in the vicinity of the AIDJEX site. These surface data consisted of measurements of ice thickness, temperature profiles, and salinity profiles at a few selected sites. In addition, extensive identifications of ice types were made over a much larger area, especially in the area of the AIDJEX strain array. Standard meteorological observations also were made continuously at the AIDJEX site, and occasionally at remote sites.

RESULTS

A photomosaic of the grid area is shown in Figure 1. The ring in the center of Figure 1 marks the location of the main AIDJEX camp, which was located on the edge of a large multiyear ice floe. Adjacent to the camp to the north was an area of smooth first-year ice which served as the aircraft landing site for the

camp. However, the differences in these ice types could not be discerned, even from the original photographs, nor could they be recognized visually from the Convair 990. Only the general pattern of leads which is partially obscured by the undercast of stratus clouds is evident in the photomosaic.

The large multiyear ice floe on which the AIDJEX camp was located is easily recognized in the 1.55 cm microwave false-color image shown in Figure 2, as a large blue (210-225 K) island in a sea of yellow (235-250 K). Surface measurements at the AIDJEX site have confirmed conclusively that the radiometrically colder areas of the scene (blue) are areas of multiyear ice and that the radiometrically warmer areas are associated with first-year ice. The AIDJEX triangular tellurometer strain array is shown in Figures 1 and 2; in situ measurements have shown that the entire strain array was on first-year ice (Hibler, et al. 1972).

Analyses of ice corings in the vicinity of the AIDJEX camp itself have shown that the camp was located on thick, multiyear ice. Also, visual observations during foot and sled traverses indicated that the large floe on which the camp was located was uniformly of multiyear structure. Both the surface-based measurements and airborne infrared radiometer temperature measurements (during the low level flights) have shown that the physical temperatures of both types of ice were equal (within 5 K), so that practically all the observed brightness temperature differences were due to the variation of the microwave emissivity of the ice. A striking feature in the lower brightness temperature, large multiyear floe, is a set of linear features formed by higher brightness temperatures and

shaped as an inverted V. This feature is easily seen in Figure 2, but is just barely distinguishable in the photomosaic (Figure 1). Evidently, this large floe had begun to break up late in the previous summer but then refroze into this present configuration. It can also be seen that the high brightness temperatures are of first-year ice and contain numerous smaller multiyear ice floes. The narrow, dark leads in Figure 1 do not appear in the microwave mosaic since they are beyond the resolution capability of the microwave radiometer.

Figure 3 shows a 1.55 cm microwave image of the same area as that shown in Figures 1 and 2, but obtained on the following day. The same patterns as in Figure 2 are evident, but brightness temperatures are generally about 8 K higher. This is attributed to the cloud cover over the entire site during that day. This brightness temperature increase is not caused by microwave emission from the clouds which is predicted to be negligible for clouds of such small liquid water content, but is attributed rather to the higher surface temperatures on the ice on a cloudy day. The lesser radiative cooling which was responsible for the higher surface temperature of the ice was confirmed by infrared measurements of the surface temperature on a portion of the low level flights during that day under the cloud cover.

The multispectral microwave brightness temperatures measured in the nadir direction during the low-level passes on the cloud-free day are shown in Figure 4. The flight line for this particular example is indicated in Figure 3, starting in the area of first-year ice and travelling generally southwestward

across the multiyear floe, particularly across the inverted V-shaped pattern of refrozen leads. The brightness temperatures from the two longest wavelength radiometers (21 and 11 cm) are essentially featureless except for an occasional simultaneous decrease of about 10-15 K which is attributed to thin ice, the order of one wavelength in thickness. At 6.0 cm, the multiyear versus first-year ice brightness temperature difference can just barely be discerned, and only after relating it to the same feature observed much more clearly by the shorter wavelength radiometers, namely, at wavelengths of 2.8 cm and shorter. Looking at the vertical and horizontal channels of the 0.81 cm radiometer, it can be seen that the multiyear ice floe shows little, if any polarization. The same was observed at 0.32 cm, but is not illustrated in Figure 4. It should be emphasized that the analysis of the large floe in the vicinity of the AIDJEX camp definitely identified the ice species as multiyear rather than glacial ice (ice island), for which polarization effects at microwave frequencies have been informally reported.

The emissivity difference between the multiyear ice and the first-year ice for the various wavelengths is in agreement with values reported earlier (Wilheit et al., 1971), generally following a linear increase with frequency, and reaching a maximum value of 0.19 at 37 GHz (0.81 cm). The measurements at 0.32 cm shown in Figure 4 are much less accurate than those at the other wavelengths because of calibration uncertainties in that particular instrument as installed in the aircraft, so we are not in a position to ascertain or refute the continuation of the linear increase of the emissivity difference to that

wavelength. The crossing of the refrozen leads which form the inverted V pattern in Figures 2 and 3 can be recognized in the low level pass shown in Figure 4 as the five large brightness temperature increases at the 0.32 and 0.81 cm wavelengths between 30 and 40 km along the track of the aircraft. To some extent, this increase can also be seen at 1.55 and 6.0 cm, but it is not as clearly defined at these longer wavelengths. Another series of brightness temperature peaks appears in the 0.81 and 0.32 cm instruments at 70 to 85 km in Figure 4. In contrast to the peaks associated with the refrozen leads at 30 and 40 km discussed above, this series is embedded in first-year rather than multiyear ice and the brightness temperature increase is much stronger at 0.32 cm than at 0.81 cm. A scrutiny of the photographs covering this area reveals that these peaks also correspond to refrozen leads. It appears that these leads have refrozen more recently than those at 30-40 km and have less snow cover than the surrounding first-year ice. Thus, the presence of snow cover on first-year ice seems to be more readily detected (by measuring the depressions between the peaks) at the 0.32 cm wavelength than at the longer wavelengths.

For comparison, the output of the nadir-viewing infrared radiometer which corresponds to the ice surface temperature has also been presented in Figure 4. Clearly, there are no thermal features which would suggest any correlation with the contrasts observed by the microwave radiometers. The only temperature features are a general cooling trend from 270 K to 260 K along the direction of the aircraft track and, about at the midpoint of the large ice floe, a sudden

temperature decrease of about 5 K. The latter decrease is attributed to a rather abrupt clearing of the overcast encountered at that point during the low-level aircraft pass over the large multiyear floe. A corresponding decrease in the sky brightness temperature was measured about two minutes (18 km) earlier by the 0.96 cm zenith-viewing radiometer and is shown in the partial record from this instrument (Figure 4) indicating a thinning of the cloud at that point.

In Figure 5, we have shown the angular dependence of the emissivity of both ice types discussed here for the 1.55 cm wavelength (horizontal component). As can be seen, the limb darkening is greater for the multiyear ice than for first-year ice.

CONCLUSIONS AND DISCUSSION

The results of these microwave and infrared airborne observations of sea ice when combined with the AIDJEX surface measurements, have demonstrated conclusively that, under typical mid-winter conditions, the microwave emissivity of multiyear ice is less than that of first-year ice and that the emissivity difference increases approximately linearly with frequency up to at least 37 GHz (0.81 cm). The emissivity of the first-year ice was close to unity for the wavelength range of 11 to 0.31 cm. For each ice type, the emissivity shows little polarization. These results certainly cannot support the prima facie conclusion that the lower salinity of multiyear ice would produce higher brightness temperatures than first-year ice. Similarly, the assumption that the greater roughness of multiyear ice, which is produced by dynamic deformations, increases its microwave emissivity is invalidated by these observations.

Questions remaining unresolved are the uniqueness of this emissivity difference with regard to the two ice types, the variation of emissivity of first-year ice with surface temperature between 260 K and the melt point, and the variation of emissivity with intermediate ice ages. Data for the last two questions will have to be obtained in subsequent missions. We have obtained some data on the first question entirely by airborne means and at separate locations from the AIDJEX activity; there appears to be at least two other ice types which have emissivities substantially lower than first-year thick sea ice, namely, first-year thin and sea ice of glacial origin. However, the variations of the emissivities of these ice types with wavelength and polarization appear to be different from the variations exhibited by thick multiyear ice. Measurements dealing with these ice types will be published separately.

A qualitative understanding of the emissivity variation in sea ice may be obtained by considering the variation of the electrical conductivity of the ice with variation in salt content which is a function of age and the scattering of microwave radiation by inhomogeneities within the ice. Thus, first-year sea ice might be considered as a lossy dielectric, and multiyear ice as a good dielectric. The skin depth in first-year ice should be in the order of a wavelength while that for multiyear ice should be many wavelengths. In the case of first-year ice, then, any emerging radiation would have to originate from within this limited skin depth; multiyear ice, on the other hand, would be transparent from much greater depths. This greater depth penetration results in considerable volume scattering

for the emerging radiation. Such volume scattering would reduce the emissivity observed above the surface and may be caused by the presence of empty brine pockets above sea level, or by the crystal structure of the ice. The exact nature of the volume scattering remains to be pursued further. This concept also explains the wavelength dependence of the emissivity because the volume scattering centers will have characteristic dimensions of the order of millimeters and will therefore scatter more strongly at shorter than at longer wavelengths. The limb darkening shown in Figure 5 is also consistent with this volume scattering concept.

ACKNOWLEDGEMENTS

The authors wish to acknowledge the use of borrowed equipment from A. Edgerton of Aerojet-General Corporation, J. C. Blinn III of Jet Propulsion Laboratory, and G. Hidy of North American (see Table I). The cooperation of W. Weeks, S. Ackley, A. Kovacs, and W. Hibler of the U.S. Army Cold Regions Research and Engineering Laboratory in obtaining the surface truth information at the AIDJEX site, P. M. Kuhn of the NOAA Environmental Research Laboratories in assisting in the processing of the infrared radiometer data and loan of his equipment, O. Smistad of NASA Manned Space Center in supplying and operating the RC-8 aerial camera, and E. V. Petersen of NASA Ames Research Center for the organization and operation of the CV990 aircraft missions is also gratefully acknowledged.

REFERENCES

A. E. Basharinov, A. S. Gurvich, S. T. Egorov, V. I. Zhukov, A. A. Kurskaya, L. I. Malafeev, D. T. Matveev, A. S. Mikhailov, and A. M. Shutko, "Results of Observation of the Thermal Radio Emission of the Earth's Surface in an Experiment on the Cosmos-243 Satellite," Kosmicheskie Issledovania 9, 268 (1971).

A. T. Edgerton, D. T. Trexler, G. A. Poe, A. Stogryn, S. Sakamoto, J. E. Jenkins, and F. Soltis, "Passive Microwave Measurements of Oceanographic Phenomena, Ice, and Sediments," Technical Report No. 9016R-7 for ONR Contract No. NOnr 4767(00) (November 1970).

K. W. Gray, W. F. Hall, W. N. Hardy, G. M. Hidy, W. W. Ho, A. W. Love, Mr. J. Van Melle, and H. Wang, "Microwave Measurement of Thermal Emission from the Sea," Proc. Seventh Int. Symp. on Remote Sensing of the Environment (Ann Arbor, May 1971).

W. Hibler, W. Weeks, S. Ackley, A. Kovac, and W. Campbell, "Mesoscale Strain Measurements on the Beaufort Sea Pack Ice," accepted for publication in the Journal of Glaciology.

P. Hoekstra and P. Cappillino, "Dielectric Properties of Sea and Sodium Chloride Ice at UHF and Microwave Frequencies," J. Geophys. Res. 76, 4922 (1971).

P. M. Kuhn, M. S. Lojko, and E. V. Petersen, "Water Vapor: Stratospheric Injection by Thunderstorms," Science 174, 1319 (1971).

D. C. Meeks, D. P. Williams, R. M. Wilcox, and A. T. Edgerton, "Microwave Radiometric Detection of Oil Slicks," Final Report No. 1335-2 for DOT Contract No. DOT-CG-93, 228A (March 1971).

A. Stogryn, D. Williams and A. T. Edgerton, "A Study of the Microwave Emission Characteristics of Sea Ice," Final Report No. 1741R-1 for DOC Contract No. 1-35139 (September 1971).

T. Wilheit, J. Blinn, W. Campbell, A. Edgerton, and W. Nordberg, "Aircraft Measurements of Microwave Emission from Arctic Sea Ice," to be published in Remote Sensing of Environment (1972).

Table I

Radiometer Characteristics

Freq. GHz	Wavelength cm	Pointing Relative to Nadir	3db Beam Width	Integration Time (seconds)	RMS Temp. Sens.	Reference
1.42	21	0°	15°	0.1	5°K	Edgerton (1970)
2.69	11	0°	27°	1.0	0.5°K	Gray (1971)
4.99	6.0	0°	5°	0.1	15°K	Edgerton (1970)
10.69	2.8	0°	7°	2.0	1.5°K	Wilheit (1972).
19.35 H	1.55	SCANNER	2.8°	0.025	1.5°K	Wilheit (1972)
31.4	0.96	180°	10°	1.0	0.9°K	Wilheit (1972)
37 V	0.81	45°	5°	0.1	3.5°K	Wilheit (1972)
37 H	0.81	45°	5°	0.1	3.5°K	Wilheit (1972)
94 V	0.32	45°	5°	0.1	7°K	Meeks (1971)
94 H	0.32	45°	5°	0.1	7°K	Meeks (1971)
INFRARED	10 microns	14°	<1°	0.1	<1°K	Kuhn (1971)

FIGURE CAPTIONS

1. Photomosaic of the test area, centered at about 74° 6'N, 131° 17'W. The aircraft altitude was 11 km; the photographs were taken on Infrared Echtachrome with an RC-8 aerial camera during the flight of March 15, 1971. The AIDJEX campsite is within the circle. The triangle indicates the AIDJEX tellurometer strain array. The area shown is about 80 km x 100 km.
2. False-color image of 1.55 cm microwave radiometer data covering the same time period and test area as shown in Figure 1, showing again the positions of the AIDJEX campsite and strain array.
3. The same as Figure 2, but taken on the following day with a complete undercast. The diagonal line passing through the campsite indicates the locations of the low-altitude run from which the data of Figure 4 were obtained.
4. Multispectral data obtained on March 16, 1971 during the low-level pass at 300 m altitude along the track indicated on Figure 3. Here, Z = zenith-viewing, H = 45° - viewing in horizontal polarization, and V = 45° - viewing in vertical polarization. The data dropouts in the 2.81 and 0.96 cm radiometers correspond to calibration cycles at those times.
5. Angular dependence of the brightness temperatures of first-year and multi-year sea ice for the horizontal component of the 1.55 cm radiation. The thermometric temperature of the surface of the ice was about 258 K. Each point represents an average over at least a 12 km-long sample of uniform sea ice along the track shown in Figure 4.

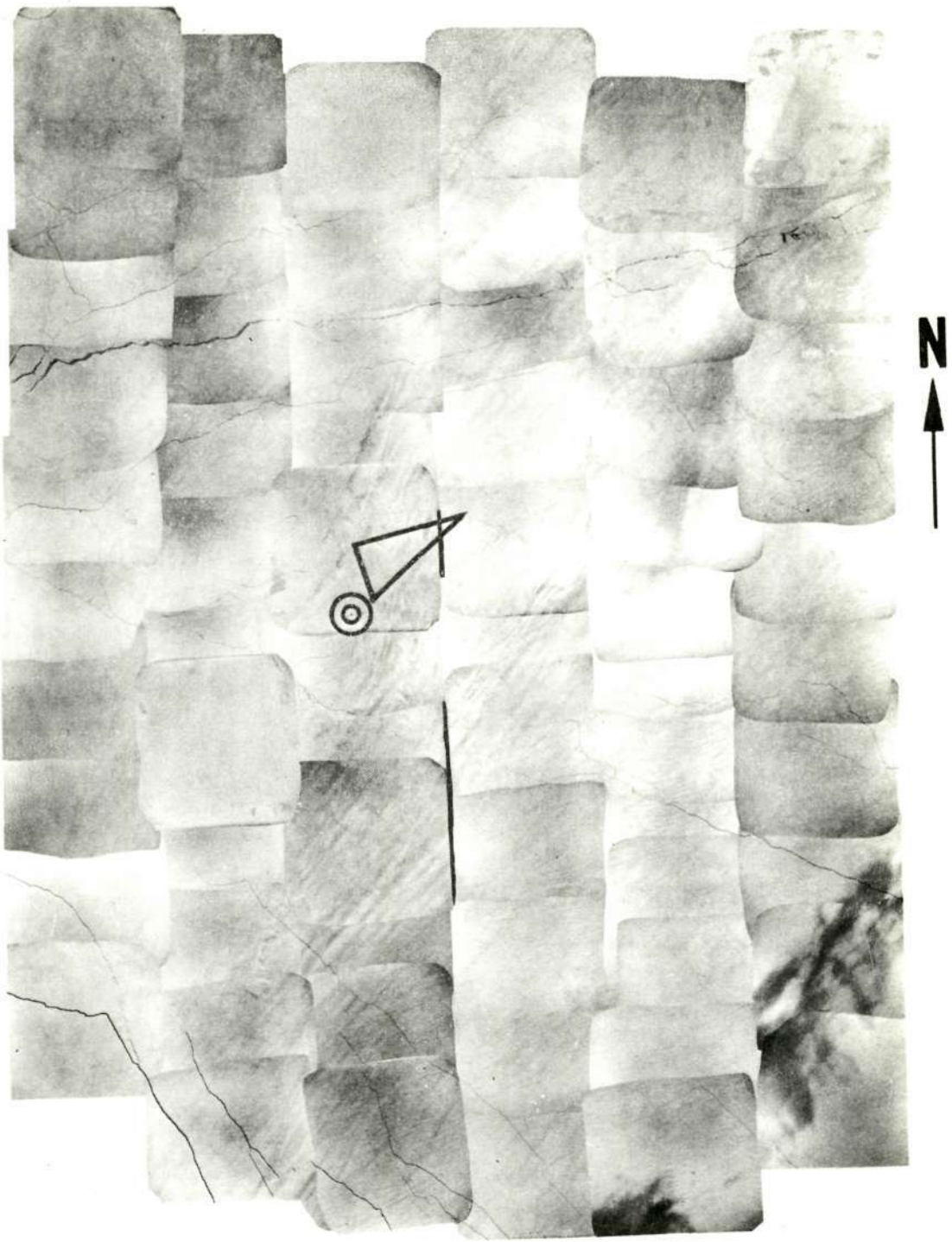

Figure 1

PASSIVE MICROWAVE IMAGE OF ARCTIC SEA ICE (λ=1.55 CM)
(NASA CV-990 AIRCRAFT, 15 MARCH 1971 - CLEAR DAY)

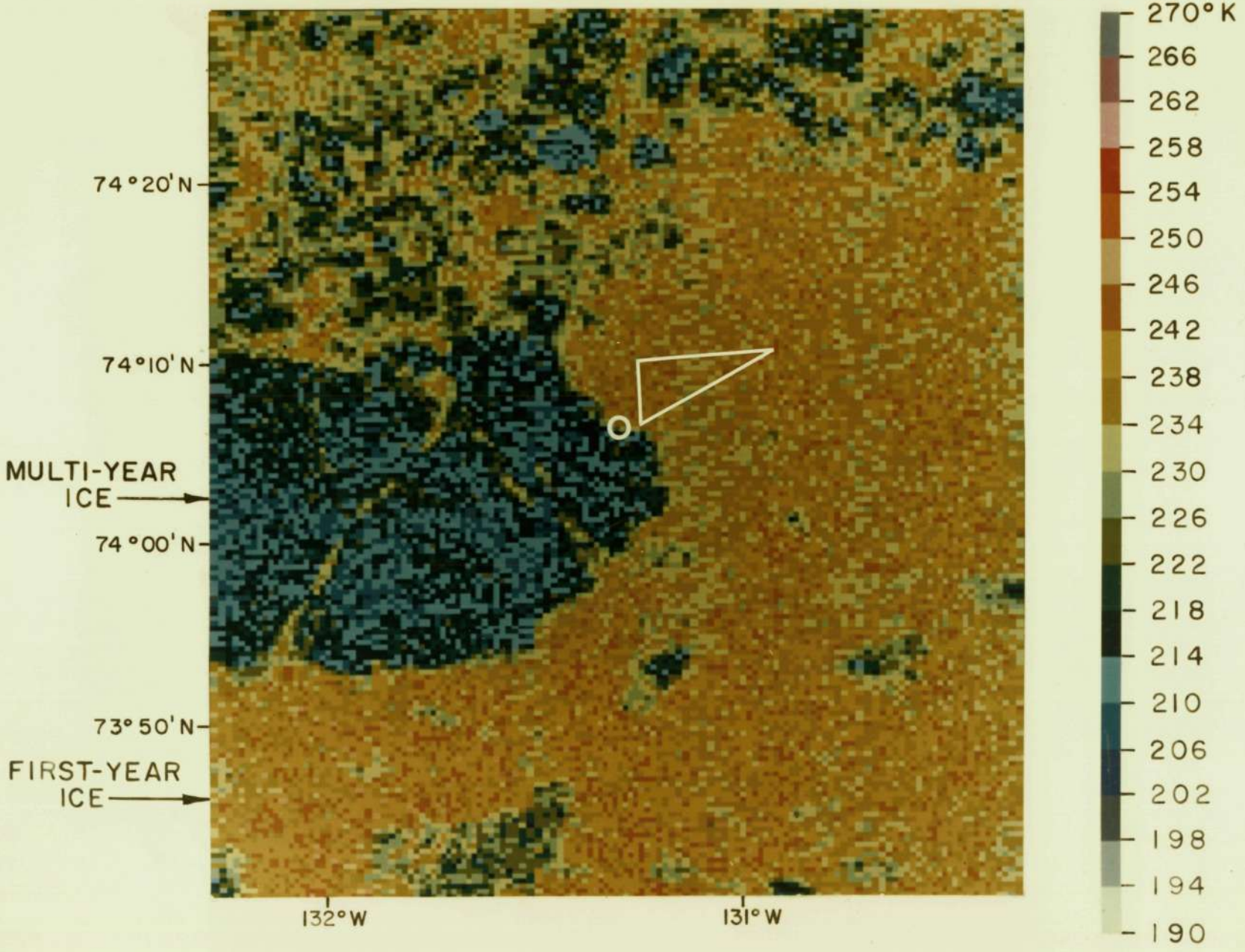

PASSIVE MICROWAVE IMAGE OF ARCTIC SEA ICE (λ=1.55 CM)
(NASA CV-990 AIRCRAFT, 16 MARCH 1971— CLOUDY DAY)

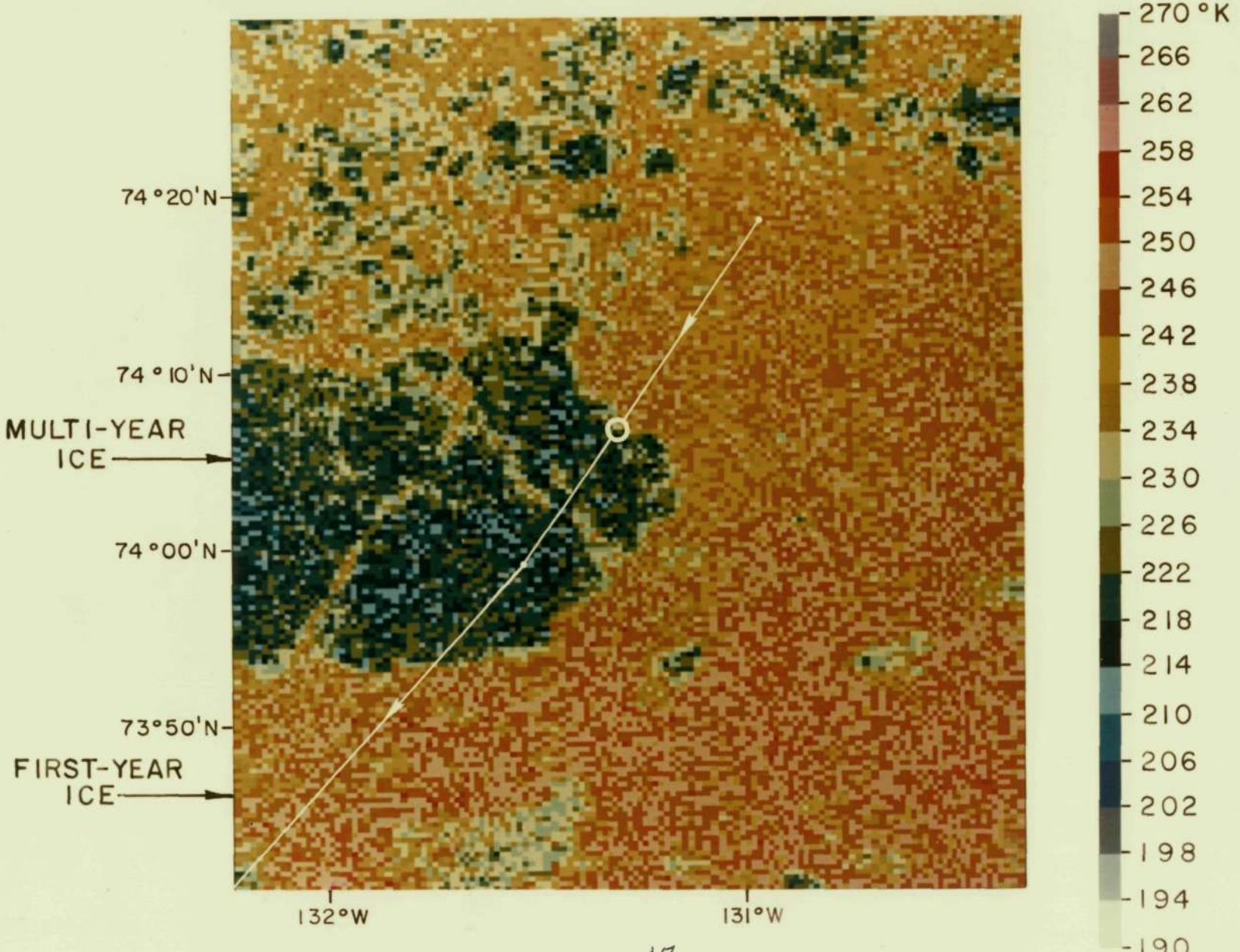

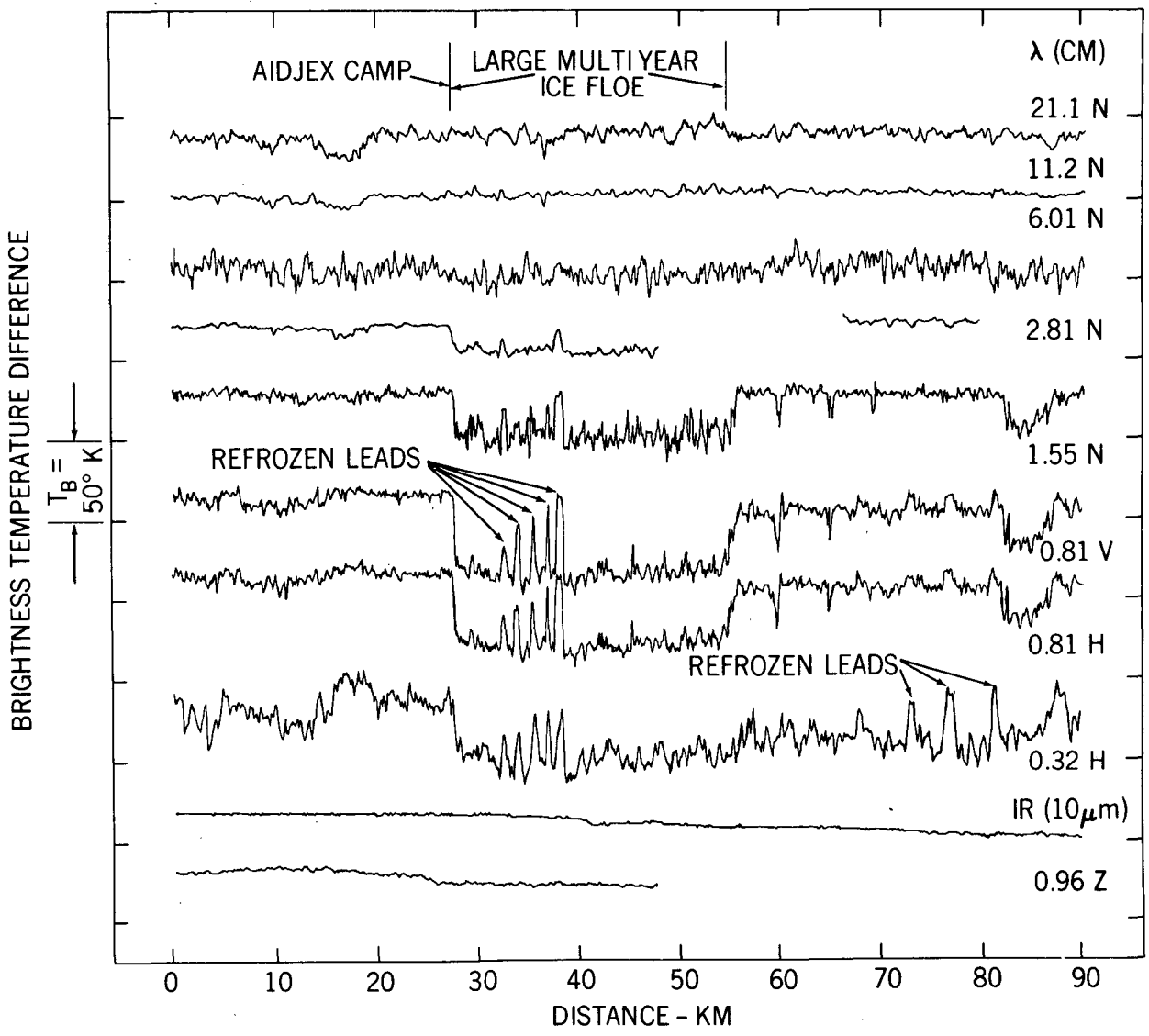
AIDJEX CAMP
LARGE MULTI YEAR ICE FLOE
λ (CM)
21.1 N
11.2 N
6.01 N
2.81 N
1.55 N
REFROZEN LEADS
0.81 V
0.81 H
REFROZEN LEADS
0.32 H
IR (10μm)
0.96 Z
BRIGHTNESS TEMPERATURE DIFFERENCE
T_B = 50° K
0
10
20
30
40
50
60
70
80
90
DISTANCE - KM

Figure 4

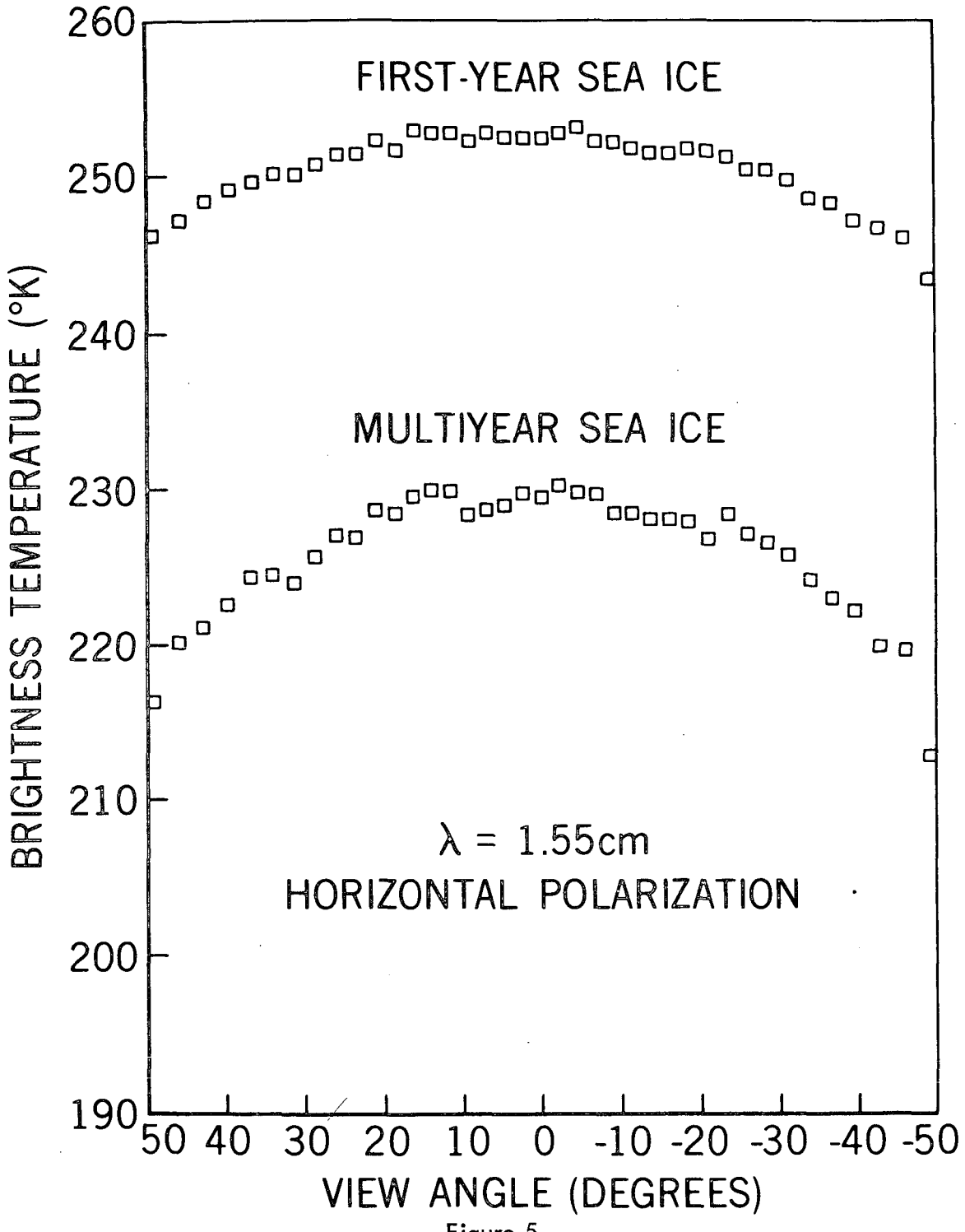
FIRST-YEAR SEA ICE
MULTIYEAR SEA ICE
λ = 1.55cm
HORIZONTAL POLARIZATION
BRIGHTNESS TEMPERATURE (°K)
260
250
240
230
220
210
200
190
50 40 30 20 10 0 -10 -20 -30 -40 -50
VIEW ANGLE (DEGREES)

Figure 5